Mechanics of the Turbulent-Nonturbulent Interface of a Jet

J. Westerweel,[*] C. Fukushima,[†] J. M. Pedersen,[‡] and J. C. R. Hunt

Laboratory for Aero and Hydrodynamics, Delft University of Technology, 2628 CA Delft, The Netherlands
(Received 17 January 2005; published 20 October 2005; corrected 24 October 2005)

We report the results of an experimental investigation of the mechanics and transport processes at the bounding interface between the turbulent and nonturbulent regions of flow in a turbulent jet, which shows the existence of a finite *jump* in the tangential velocity at the interface. This is associated with small-scale eddying motion at the outward propagating interface (nibbling) by which irrotational fluid becomes turbulent, and this implies that large-scale engulfment is *not* the dominant entrainment process. Interpretation of the jump as a singular structure yields an essential and significant contribution to the mean shear in the jet mixing region. Finally, our observations provide a justification for Prandtl's original hypothesis of a *constant* eddy viscosity in the nonturbulent outer jet region.

In free-shear turbulent flows, such as turbulent wakes, shear layers, and jets, the turbulent flow region is bounded by nonturbulent (viz., irrotational) fluid. The sharp interface between the turbulent and nonturbulent flow regions is strongly contorted over length scales proportional to the integral length scale and propagates into the irrotational flow region while irrotational fluid is entrained into the turbulent flow region. A long-standing problem about these unconfined, but localized, turbulent flows is to describe and quantify the characteristic features of the inhomogeneous interface [1–4], and to identify the nature of the entrainment process by which irrotational fluid becomes turbulent. It has been unclear whether this occurs as the result of outward spreading of small-scale vortices ("nibbling") or large-scale engulfment by the inviscid action of the dominant eddies in the turbulent flow region. Recent results obtained from numerical simulations indicate that engulfment is not the dominant process [5], in contrast to conclusions from many earlier studies [2,6].

In this Letter we describe experimental findings on the mechanics and transport processes at the turbulent-nonturbulent interface of a turbulent jet. Most notably we observe a finite jump in the tangential velocity at the jet interface. The experimental data also show that engulfment makes only a small contribution to the jet mass flux, that the velocity fluctuations relative to the interface have a typical length scale of the order of the Taylor microscale, and that the turbulent (viz., inviscid) enstrophy flux at the interface does not contribute to the outward propagation of the interface. These results have general implications for the proper modeling of turbulence at the turbulent-nonturbulent interface.

The experimental setup consists of a water-filled rectangular $110 \times 110 \times 300$ mm^3 test section. A syringe pump drives the jet fluid into the test section through a $d = 1$ mm inner diameter nozzle with a mean velocity of 2 m/s, so that the jet Reynolds number is 2×10^3. The fluid motion is measured by means of combined velocity and concentration measurements in a planar cross section through the jet center line [7,8]. Planar *laser-induced fluorescence* (LIF) is used to visualize the jet fluid that has been labeled with a fluorescent dye (disodium fluorescein), and *particle image velocimetry* (PIV) to simultaneously measure the instantaneous velocity field from the motion of small (5 μm) tracer particles suspended in the fluid. A combination of optical filters and proper timing of the laser illumination prevents mutual influence of the LIF and PIV images, which are each recorded by a separate camera on opposite sides of the light sheet plane [7,8]. The cameras have a 922×1004-pixel resolution, and the PIV images were originally interrogated in 32×32-pixel domains [7,8] and for the present analysis in 16×16-pixel domains with 8-pixel spacing.

Analysis of the velocity and concentration results at several locations between 30 and 140 nozzle diameters show that the jet is self-similar [7]. For the analysis of the flow relative to the jet interface we used the data between 60 and 100 nozzle diameters, where a total of 657 combined PIV-LIF images were recorded. The dye has such a high Schmidt number (Sc $= 2 \times 10^3$) that molecular diffusion is negligible and the interface remains sharp. Applying a threshold detection [9] on the LIF concentration data yields the jet interface. Where the interface is strongly convoluted and irrotational fluid is being engulfed, we consider only the outer interface contour, which we refer to as the interface *envelope;* see Fig. 1(a). Details of this procedure are given in [8]. The PIV velocity data are conditionally sampled with respect to the position of the interface envelope [10]; by following the envelope, engulfed flow regions that may contaminate the results are excluded from the conditional averaging. The mean conditional out-of-plane component of the vorticity $\langle \Omega_z \rangle$ [11], computed from the two in-plane velocity components, is shown in Fig. 1(b). This component of the vorticity vector is dominant at the bounding interface [10,12]. When the profiles are scaled with the center-line velocity and the jet half-width, the conditional profiles are self-similar [Fig. 1(c)]. In contrast to the gradual decay of the mean vorticity in a laboratory frame, the mean conditional vorticity shows a sharp change at the interface with a more or
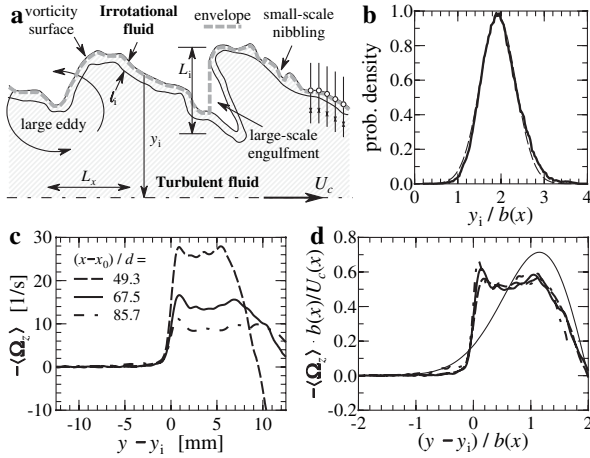
FIG. 1.   (a) The turbulent-nonturbulent interface for a jet. The vertical lines on the right indicate the conditional averaging with respect to the interface; after Bisset *et al.* [10]. The gray dashed line defines the interface envelope as the outer interface contour. (b) The PDF of the interface position y_i is approximately Gaussian with a mean of $1.97b$ and standard deviation of $0.41b$. (c) The mean conditional vorticity $\langle \Omega_z \rangle$ as a function of the distance from the interface at y_i at three different distances from the nozzle. (d) As in (c), but now $\langle \Omega_z \rangle$ has been scaled with the jet mean half-width $b(x)$ and mean center-line velocity $U_c(x)$. The thin line represents the mean vorticity profile with respect to the center line.

less constant value in the turbulent flow region. A small peak is observed at the interface. This peak is broadened by the finite resolution of the PIV, but indicates the existence of a "jump" at the interface that can be associated with a thin shear layer, or "superlayer" [13]. The existence of a jump ΔU in the tangential velocity is consistent with a control-volume analysis [14] for the momentum at the interface that propagates at a finite velocity E_b into the irrotational flow region, given by $E_b \Delta U = -F_\tau$, where F_τ is the momentum flux [Fig. 2(a)]. Conclusions drawn from early attempts to measure ΔU from conditionally sampled hot-wire data [15] were not substantiated by the data. Ever since, the existence of this jump has been debated [3,14].

In Figs. 2(b) and 2(c) are shown the profiles of the conditional mean axial velocity and the conditionally sampled Reynolds stress. Figure 2(d) shows an enlargement of the profile of $\langle U \rangle$ in Fig. 2(b). Indeed, a small jump can be observed, though it is somewhat blurred by the combined result of finite fluid viscosity and finite PIV spatial resolution. The jump is estimated at $0.09U_c$ and the jump in the conditional Reynolds stress at $0.0066U_c^2$, which yields a value of $E_b = 0.07U_c$. This value for the interface propagation velocity is in agreement with the jet entrainment velocity $E = -2\langle V \rangle$ [16], where $\langle V \rangle$ is the mean inward radial velocity at the jet interface, which is $\langle V \rangle = 0.035U_c$ in our experiments.

If the entrainment would be a purely inertial process, then the outward propagation ($v < 0$) of enstrophy $\langle \omega_z^2 \rangle$ carries turbulent fluid into the irrotational flow region, whereas the inward propagation ($v > 0$) carries irrotational
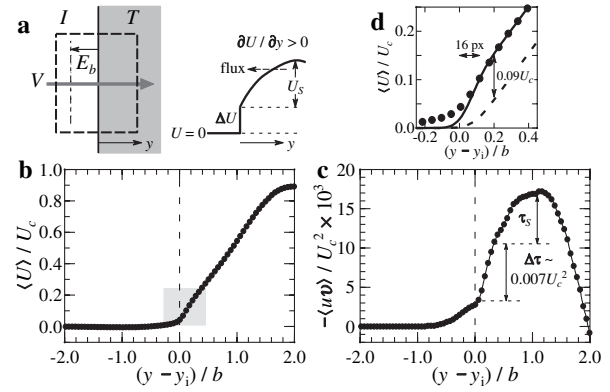

FIG. 2.   (a) Idealized control-volume analysis for the tangential momentum at the interface separating irrotational (*I*) and turbulent (*T*) flow domains. Propagation of the interface into *I* at a rate E_b implies a finite jump ΔU in the tangential velocity (a similar condition applies to the conditional Reynolds stress). (b),(c) The profiles of the mean conditional axial velocity $\langle U \rangle$ and the conditional Reynolds stress $\langle uv \rangle$. (d) Detail of (b); the dashed and solid lines represent model velocity profiles for $\Delta U = 0$ and $0.09U_c$, respectively (the model includes the finite 16-px spatial resolution of the PIV data).

fluid into the turbulent region [Fig. 3(a)], so that the averaged net difference is a positive (viz., outward) flux of enstrophy, i.e., $-\langle v \omega_z^2 \rangle > 0$. Figure 3(b) contains an example of the instantaneous enstrophy flux along the jet envelope, showing strongly intermittent behavior in which the instantaneous enstrophy flux can attain large values. The large spikes mainly occur in pairs that can be associated with engulfment events [Fig. 3(a)]. However, when the data are scaled and averaged over all measurements, the PDF for $v\omega_z^2$ [Fig. 3(c)] has a narrow symmetric peak that yields a zero mean value for the enstrophy flux, i.e., the net
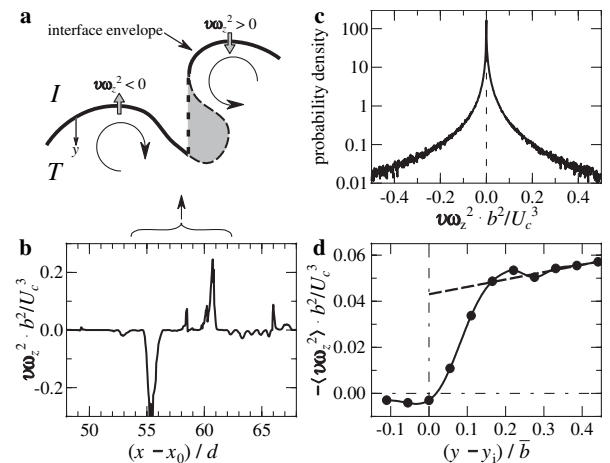

FIG. 3.   Turbulent enstrophy transport at the interface. (a),(b) Instantaneous enstrophy transport at the interface; fluctuation pairs of opposite sign correspond to engulfment events. (c) The PDF for $v\omega_z^2$ at the interface. (d) The conditional enstrophy transport $\langle v\omega_z^2 \rangle$ along lines parallel to the interface (symbols correspond to the 8-pixel PIV data spacing).

contribution of the turbulent enstrophy flux to the propagation of the interface is zero. Hence, the inertial flux does not transport any vorticity across the interface. Figure 3(d) shows the enstrophy flux obtained along lines parallel to the interface, which indicates that the turbulent flux is responsible for the transport of enstrophy towards the interface within a distance of $0.1b$, which is of the order of the Taylor microscale.

The jet envelope has been defined as the outer contour of the jet interface, and, in regions where the interface is convoluted, irrotational fluid is found within the jet envelope [Fig. 3(a)]. This fluid can be defined as the amount of engulfed fluid. The number of pixels within the jet envelope can be used to estimate the total jet mass, and the number of pixels that contain irrotational fluid can be used to estimate the fraction of irrotational fluid mass within the jet [5] [Fig. 4(a)]. When integrated over y and multiplied by U_c, these data yield estimates for the total jet mass flux $\dot{Q}$ and the contribution of engulfed irrotational fluid $\dot{Q}_e$; see Fig. 4(b). It appears that the relative contribution of engulfment to the total jet mass is only 7%–10%; this experimental result is in agreement with the result from a numerical simulation of a time-evolving jet [5]. Our observation that the entrainment is not determined by large-scale engulfment and that a small-scale process occurs at the jet boundary implies the mixing transition described by Dimotakis [17] has occurred before the observed flow region (between 60 and 100 nozzle diameters) of our Re = 2×10^3 jet. Note that the probability of the existence of irrotational fluid at the jet center line, i.e., $p_e(\eta = 0)$, is *finite* [Fig. 4(a)], so our observation that engulfment is not dominant does *not* preclude the penetration of irrotational fluid far into the jet.

To obtain additional information about the dominant length scales at the jet interface, we determined the spatial autocorrelation of the conditional axial velocity fluctuations along lines parallel to the jet interface, and then integrated the spatial correlations to obtain estimates of the integral length scales. The results are shown in Fig. 5. The length scales obtained from the resampled conventional velocity fluctuations are more or less constant, in agreement with existing experimental data [18]. The result
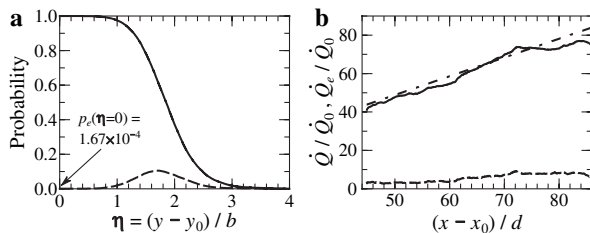
for the integral length scale from the conditional fluctuations has a minimum at the interface that is close to the Taylor microscale (estimated at $0.1b$), and supports our earlier conclusion that small-scale nibbling is the dominant process at the jet interface.

The superlayer jump is associated with an asymptotic singularity in the conditional vorticity profile (for Re $\rightarrow$ ∞). Although our data are taken at a single and finite Reynolds number, the jump is interpreted in terms of a singular structure. The existence of a singularity in the scalar gradient at the interface is well established (e.g., [19]), and this can be extended to the existence of a singularity in $\langle \Omega_z \rangle$ [10]:

$$\langle \Omega_z \rangle(n) \approx H(n) \frac{\partial \langle U \rangle}{\partial n} + \delta(n) \Delta U, \qquad (1)$$

where n is the coordinate normal to the interface, and $\delta(s)$ and $H(s)$ the Dirac δ-function and step function, respectively. Convolution of the observed profiles for the conditional vorticity and Reynolds stress with the PDF of y_i [Fig. 1(b)] yields the conventional profiles for the mean vorticity and the Reynolds stress. To calculate the vorticity Ω_z in a *laboratory frame* relative to the mean interface position $\bar{y}_i$, we use the experimental result that the interface position y_i has a normal distribution with a mean $\bar{y}_i = 1.93b$ and standard deviation $\sigma_i = 0.41b$ [Fig. 1(b)]. This yields

$$\Omega_z(\Delta_y) \cong \underbrace{\frac{1}{2} \frac{\partial \langle U \rangle}{\partial n} \left[1 + \mathrm{erf}\left(\frac{\Delta_y}{\sigma_i \sqrt{2}} \right) \right]}_{A(\Delta y)} + \underbrace{\frac{\Delta U_i}{\sigma_i \sqrt{2\pi}} \exp\left(\frac{\Delta y^2}{2\sigma_i^2} \right)}_{B(\Delta y)}$$
$$(2)$$

where $\Delta y = y - \bar{y}_i$. The convolution is corrected for the fact that the envelope is defined as the outer position of the interface and that a small fraction of irrotational fluid is contained within the jet. This fraction is about 0.27 at $y = \bar{y}_i$ [i.e., $\eta = 1.93$; see Fig. 4(a)]. The predicted vorticity profile is in excellent agreement with experimental data (Fig. 6). Note that the dashed line represents the model prediction *without* the singularity at the interface, i.e.,

FIG. 4. (a) Probability of the existence of jet fluid (solid line) and entrained fluid (dashed line) as a function of the normalized distance η from the jet center line. (b) The total mass flux (solid line) and mass flux of entrained irrotational fluid (dashed line) within the outer jet boundary. The straight line (dash-dotted line) is proportional to $U_c b^2$.
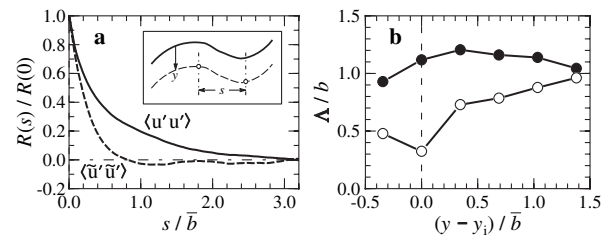

FIG. 5. (a) The conditional spatial correlation $R(s)$ of the axial velocity fluctuations along lines parallel to the interface (inset). Results for $R(s)$ at the interface ($y = y_i$) for fluctuations u' defined with respect to $\bar{U}$ (solid line) and for fluctuations $\tilde{u}'$ defined with respect to $\langle U \rangle$ (dashed line). (b) Integral length scale $\Lambda = \int R(s)ds/R(0)$ as a function of the distance from the interface for $\langle u'u' \rangle$ (solid symbols) and $\langle \tilde{u}'\tilde{u}' \rangle$ (open symbols).
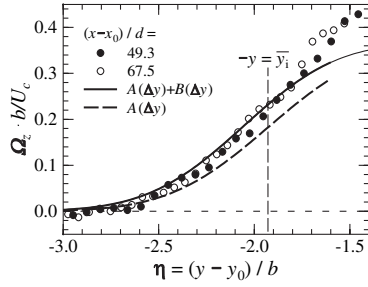
FIG. 6. Comparison of (2) with experimental data for Ω_z; exclusion of $B(\Delta y)$ (associated with the viscous shear layer) yields a significant underestimation of the experimental data.

$\partial \bar{U}/\partial y = A(\Delta y)$. This significantly underpredicts the vorticity profile. The addition of the singularity in our model (1) yields the correct quantitative prediction of the vorticity profile and confirms the significance of the interface shear layer in $\langle \Omega_z \rangle$ [Figs. 1(b) and 1(c)] and the observed jump in $\langle U \rangle$ [Fig. 2(d)].

Similar to $\langle \Omega_z \rangle$, the conditional Reynolds stress $\langle uv \rangle$ can be modeled by means of a step function, i.e., $\langle uv \rangle = \Delta \tau H(n)$, where $\Delta \tau$ is the jump at the interface. Convolution with the PDF for y_i yields an expression for $\overline{uv}$ with a form similar to $A(\Delta y)$. Thus, the ratio $\overline{uv}/\frac{\partial \bar{U}}{\partial y}$ $(= \nu_T)$ yields a *constant* eddy viscosity for the outer region of the jet, with a value $\nu_T = \Delta \tau / (\partial \langle U \rangle / \partial n) \approx 0.013 U_c b$. Thus, the eddy viscosity (defined in *laboratory* coordinates) is *finite,* even though the turbulence is decreasing to zero outside the shear layer; a nonzero eddy viscosity appears in disagreement with the absence of turbulence in this region. However, a zero eddy viscosity implies $\Delta \tau \rightarrow 0$ and consequently that $E_b = 0$. To overcome this unphysical condition, turbulence models usually make some assumption about a finite "background" value for ν_T [3,20]. However, for our *conditional* data the eddy viscosity vanishes in the irrotational (i.e., nonturbulent) flow domain, yet at the same time predicts a nonzero constant eddy viscosity defined in *laboratory* coordinates. Hence, a surprising conclusion is that the original Prandtl-Goertler solution [18], which assumes a constant eddy viscosity over the full flow domain, appears to give a more correct physical description than "advanced" models in which $\nu_T \rightarrow 0$ in irrotational flow domains.

We conclude that there is a superlayer jump for the tangential velocity component as predicted by a control-volume analysis for the momentum at the interface. The interface location could be determined unambiguously from the measured concentration field of a dye with a large Schmidt number. The small velocity jump is associated with an asymptotic singularity (for Re $\rightarrow \infty$) in the mean conditional vorticity. Engulfment of irrotational fluid is not the dominant process for the entrainment of irrotational fluid in a turbulent jet, which confirms the results from a numerical analysis [5]. This is a striking difference with conclusions from earlier studies in boundary layers and mixing layers, where engulfment was identified as the

dominant process [2,6]. The observed length scales at the interface indicate that the fluid motion at the interface is dominated by viscous interaction with a length scale of the order of the Taylor microscale. This is supported by the observation that the turbulent enstrophy flux has a zero net contribution to the transport of enstrophy at the interface. The implication of the observed profiles for the conditional vorticity and Reynolds stress for the modeling of free-shear turbulence at the turbulent-nonturbulent interface is that the eddy-viscosity has a nonzero and constant value in the irrotational outer flow region (in *laboratory* coordinates); thus, there exists a remarkable physical basis for Prandtl's initial hypothesis.

*Electronic address: J.Westerweel@wbmt.tudelft.nl
†Present address: Department of Mechanical Systems Engineering, Hiroshima Institute of Technology, Hiroshima, Japan.
‡Present address: Department of Mechanical Engineering, Technical University of Denmark, Lyngby, Denmark.

[1] J. O. Hinze, *Turbulence* (McGraw-Hill, New York, 1975).
[2] A. A. Townsend, *The Structure of Turbulent Shear Flow* (Cambridge University Press, Cambridge, U.K., 1976), 2nd ed.
[3] J. C. R. Hunt, N. D. Sandham, J. C. Vassilicos, B. E. Launder, P. A. Monkewitz, and G. F. Hewitt, J. Fluid Mech. **436**, 353 (2001).
[4] A. Tsinober, *An Informal Introduction to Turbulence* (Kluwer, Dordrecht, 2001).
[5] J. Mathew and A. Basu, Phys. Fluids **14**, 2065 (2002).
[6] G. L. Brown and A. Roshko, J. Fluid Mech. **64**, 775 (1974).
[7] C. Fukushima, L. Aanen, and J. Westerweel, in *Laser Techniques for Fluid Mechanics*, edited by R. J. Adrian *et al.* (Springer, Berlin, 2002), pp. 339–356.
[8] J. Westerweel, T. Hofmann, C. Fukushima, and J. C. R. Hunt, Exp. Fluids **33**, 873 (2002).
[9] R. R. Prasad and K. R. Sreenivasan, Exp. Fluids **7**, 259 (1989).
[10] D. K. Bisset, J. C. R. Hunt, and M. M. Rogers, J. Fluid Mech. **451**, 383 (2002).
[11] For brevity the "out-of-plane component of the vorticity" will simply be referred to as "vorticity."
[12] T. Hori and J. Sakakibara, Meas. Sci. Technol. **15**, 1067 (2004).
[13] S. Corrsin and A. L. Kistler, NACA, Washington DC, Technical Report No. 1244, 1955.
[14] W. C. Reynolds, J. Fluid Mech. **54**, 481 (1972).
[15] L. S. G. Kovasznay, V. Kibens, and R. F. Blackwelder, J. Fluid Mech. **41**, 283 (1970).
[16] J. S. Turner, J. Fluid Mech. **173**, 431 (1986).
[17] P. E. Dimotakis, J. Fluid Mech. **409**, 69 (2000).
[18] N. Rajaratnam, *Turbulent Jets* (Elsevier, Amsterdam, 1976).
[19] M. G. Mungal and D. K. Hollingsworth, Phys. Fluids A **1**, 1615 (1989).
[20] J. B. Cazalbou, P. R. Spalart, and P. Bradshaw, Phys. Fluids **6**, 1797 (1994).